Development 137, 2539-2550 (2010) doi:10.1242/dev.048371

Neuronal Nogo-A regulates neurite fasciculation, branching and extension in the developing nervous system

Marija M. Petrinovic[1,*,†], Carri S. Duncan[1,*], Dimitris Bourikas[2], Oliver Weinman[1], Laura Montani[1], Aileen Schroeter[1], David Maerki[3], Lukas Sommer[3], Esther T. Stoeckli[2] and Martin E. Schwab[1]

SUMMARY

Wiring of the nervous system is a multi-step process involving complex interactions of the growing fibre with its tissue environment and with neighbouring fibres. Nogo-A is a membrane protein enriched in the adult central nervous system (CNS) myelin, where it restricts the capacity of axons to grow and regenerate after injury. During development, Nogo-A is also expressed by neurons but its function in this cell type is poorly known. Here, we show that neutralization of neuronal Nogo-A or Nogo-A gene ablation (KO) leads to longer neurites, increased fasciculation, and decreased branching of cultured dorsal root ganglion neurons. The same effects are seen with antibodies against the Nogo receptor complex components NgR and Lingo1, or by blocking the downstream effector Rho kinase (ROCK). In the chicken embryo, in ovo injection of anti-Nogo-A antibodies leads to aberrant innervation of the hindlimb. Genetic ablation of Nogo-A causes increased fasciculation and reduced branching of peripheral nerves in Nogo-A KO mouse embryos. Thus, Nogo-A is a developmental neurite growth regulatory factor with a role as a negative regulator of axon-axon adhesion and growth, and as a facilitator of neurite branching.

KEY WORDS: Branching, Chick, Fasciculation, Mouse, Neurite outgrowth, Nogo-A, Repulsion

INTRODUCTION

Developing neurons send out processes that reach their targets guided mostly by extracellular cues that are either permissive, attractive and growth promoting, or repulsive and inhibitory (Chilton, 2006; Dickson, 2002; Huber et al., 2003). Several evolutionarily conserved families of guidance and cell adhesion molecules have been identified (Chilton, 2006; Dickson, 2002; Huber et al., 2005). Selective fasciculation and defasciculation regulated by interaxonal adhesion and repulsion from surrounding tissues help to define accurate axonal projections, e.g. by cell adhesion molecules (CAMs) on the surface of axons (Rutishauser, 2008; Van Vactor, 1998). Thus, spatial and temporal modulation of neural cell adhesion molecule (NCAM) activity by polysialic acid (PSA) regulates sorting of motor axons and peripheral nerve formation during innervation of the vertebrate limb (Rafuse and Landmesser, 2000). Ephrins, semaphorins and slits are thought to promote fasciculation by creating a repulsive environment that channels axons and prevents them from entering into non-target areas (Chilton, 2006; Eberhart et al., 2000; Huber et al., 2005). Removal of these repulsive cues or their neuronally expressed receptors leads to defasciculation and guidance errors.

An important growth cone collapsing and growth inhibitory protein in the adult central nervous system (CNS) is Nogo-A (also known as Rtn4). The protein is mainly known for its inhibitory effects on axon regeneration and compensatory sprouting after CNS injury (Schwab, 2004; Yiu and He, 2006). In the adult CNS Nogo-A is expressed primarily by oligodendocytes and myelin (Caroni and Schwab, 1988; Huber et al., 2002; Wang et al., 2002). Nogo-A affects the cytoskeleton by binding to a receptor complex containing NgR (also known as Rtn4r), p75/TROY and Lingo1, and activating the small GTPase RhoA and ROCK (Fournier et al., 2003; Montani et al., 2009; Yiu and He, 2006). In addition to its glial expression in the adult, Nogo-A is expressed by many peripheral and central neurons during development (Huber et al., 2002; Hunt et al., 2003; Josephson et al., 2001; Wang et al., 2002). An early developmental role in the restriction of migration of cortical interneurons has been described (Mingorance-Le Meur et al., 2007). Later in development, Nogo-A is involved in restricting plasticity in the visual cortex and other parts of the CNS (Kapfhammer and Schwab, 1994; McGee et al., 2005).

Here, we show that suppression of Nogo-A signalling leads to increased neurite outgrowth, increased fasciculation, and decreased branching in cultured dorsal root ganglion (DRG) neurons. In the chicken embryo, in ovo injection of function-blocking anti-Nogo-A antibodies led to highly bundled peripheral nerves with reduced branching. Similar changes were observed in Nogo-A knock-out (KO) mouse embryos. These observations suggest that Nogo-A acts as a negative regulator of axon-axon adhesion contributing to the regulation of fasciculation and the branching of fibre tracts during nervous system development.

MATERIALS AND METHODS

Animals

Embryonic and newborn (P0-P1) C57Bl/6 wild-type and Nogo-A KO mice, C57BL/6-Tg(ACTB-EGFP)1Osb/J mice (Jackson; eGFP cDNA under the control of a chicken β-actin promoter), neonatal Wistar rats, and embryonic chicks were used in this study. All animal experiments were performed according to the guidelines of the Veterinary Office of the Canton of Zürich, Switzerland, and approved by its Commission for Animal Research.

[1]Brain Research Institute, University of Zurich and Department of Biology, ETH Zurich, Winterthurerstrasse 190, 8057 Zurich, Switzerland. [2]Institute of Zoology, University of Zurich, Winterthurerstrasse 190, 8057 Zurich, Switzerland. [3]Cell and Developmental Biology, Institute of Anatomy, University of Zurich, Winterthurerstrasse 190, 8057 Zurich, Switzerland.

*These authors contributed equally to this work
†Author for correspondence (petrinovic@hifo.uzh.ch)

Accepted 18 May 2010

Nogo-A KO mice were generated by homologous recombination of exons 2 and 3 in the Nogo-A gene, as described previously (Dimou et al., 2006; Simonen et al., 2003).

Antibodies

11C7 antibody was raised against an 18-amino acid Nogo-A peptide corresponding to the rat sequence of amino acids 623-640 (Oertle et al., 2003). 7B12 antibody has an epitope in the C-terminal part of the Nogo-A-specific region (aa 763-820) (Oertle et al., 2003). Both antibodies are function-blocking antibodies (Liebscher et al., 2005) and are monospecific for Nogo-A (Dodd et al., 2005; Oertle et al., 2003). Polyclonal rabbit antibody Rb173A (Laura) recognizes the Nogo-A-specific region (aa 174-979) and the antibody Rb1 (Bianca) is specific for the N terminus of Nogo-A and Nogo-B (aa 1-172) (Dodd et al., 2005; Oertle et al., 2003). Nogo-A receptor complex components were blocked by anti-NgR (R&D Systems) or anti-Lingo1 (Abcam) antibodies. Compound Y27632 was used to inhibit ROCK (Sigma). Rabbit anti-neurofilament 160 antibody (Chemicon) was used for whole-mount staining and mouse anti-β-tubulin III (Abcam) was used for staining of dissociated DRG cultures.

DRG cultures

DRG explant cultures

DRGs of newborn rats, wild-type and Nogo-A KO mice were plated on 20 μg/ml poly-L-lysine (PLL)-coated four-well tissue culture plates. Cultures were incubated for 5-7 days at 37°C and 5% CO_2 atmosphere in F12 medium (Invitrogen) supplemented with 10% foetal bovine serum (Sigma), 100 μg/ml nerve growth factor (NGF) and 10 μg/ml gentamycin (Sigma). Cytosine arabinoside was added to inhibit mitosis of non-neuronal cells. Control, monoclonal mouse IgG antibody directed against wheat auxin, anti-Nogo-A antibodies 11C7 or 7B12, antibodies against NgR-1 or Lingo1 or the ROCK blocker Y27632 were added to the culture medium at a concentration of 10 μg/ml at the beginning of the culturing period.

Dissociated DRG cultures

DRG neuron cultures of newborn wild-type and Nogo-A KO mice were prepared as previously described (Montani et al., 2009).

Transduction of primary DRG neurons

Neonatal Nogo-A KO mouse DRG neurons were infected at the time of plating for 10-24 hours with either AAV2.eGFP or AAV2.Nogo-A at a multiplicity of infection (MOI) of 1. Transduction efficiency was assessed by immunostaining against either eGFP or Nogo-A.

Electron microscopy

Transmission and scanning electron microscopy experiments were performed as described previously (Aloy et al., 2006; Rutishauser et al., 1978).

Immunoblotting

Western blots of mouse brain lysates and DRG neurons were carried out as previously described (Montani et al., 2009) and, for quantification, protein band intensities were normalized to GAPDH values.

Quantitative real-time PCR

DRGs from mice of different ages ranging from E15-P60 were rapidly dissected in RNAlater solution (Ambion). The RNA was prepared with the RNeasy Micro Kit (QIAGEN). Residual genomic DNA was digested by DNase treatment. For reverse transcription, the same amounts of total RNA were transformed by oligo-dT and M-MLV reverse transcriptase (Promega). For all tissues, cDNAs corresponding to 5 ng of total RNA were amplified with specific primers designed to span intronic sequences or to cover exon-intron boundaries.

Primers specific for NgR (forward, 5′-CTCGACCCCGAAGATGAAG; reverse, 3′-TGTAGCACACACAAGCACCAG) were used. Gene expression was analyzed by real-time reverse transcription (RT)-PCR with a polymerase ready mix (LightCycler 480; SYBR Green I Master; Roche Diagnostics) and a thermocycler (LightCycler; Roche). Analysis of the melting curve of each amplified PCR product and visualization of the PCR amplicons on 1.5% agarose gels allowed the specificity of the amplification to be controlled. For relative quantification of gene expression, mRNA levels were normalized to glyceraldehyde-3-phosphate dehydrogenase (GAPDH) and β-actin using the comparative threshold cycle ($\Delta\Delta^{CT}$) method. Each reaction was carried out in triplicate.

Time-lapse video microscopy

Images were taken with a cooled digital CCD Hamamatsu Orca camera attached to the inverted widefield Leica DM IRBE microscope equipped with a 10× phase contrast objective (NA 0.3) and an environmental chamber maintained at 37°C and 5% CO_2 atmosphere. Images were acquired every 5 minutes over an observation period of 10-20 hours and subsequently assembled into movies with the OpenLab 3.1.7 and QuickTime (Apple) (0.10 seconds/frame) software.

Immunofluorescence staining of DRG neurons

Surface staining

Dissociated DRGs were plated on PLL- and laminin-coated glass coverslips. After 24 hours in culture, living cells were washed with room temperature PBS and subsequently transferred on a cold metal plate (10-14°C), where they were rinsed with cold PBS containing 1 mM $CaCl_2$ and 0.5 mM $MgCl_2$. After the blocking step, primary antibody (anti-Nogo-A Ab Rb173A; anti-Phaseolus vulgaris agglutinin) diluted to 100 μg/ml in cold blocking TNB buffer (0.1 Casein, 0.25% BSA, 0.25% TopBlock in TBS) was added to live cells for 20 minutes. After rinsing with cold TBS cells were fixed with 4% paraformaldehyde (PFA) for 20 minutes at room temperature. Following incubation with secondary antibody, FITC-conjugated streptavidin was applied for 30 minutes. The cells were then washed three times with TBS and mounted on slides with Mowiol [10% Mowiol 4-88 (w/v) (Calbiochem) was dissolved in 100 mM Tris (pH 8.5) with 25% glycerol (w/v), and 0.1% 1,4-diazabicyclo[2.2.2]octane (DABCO) was added as an anti-bleaching reagent].

Confocal imaging was performed using a Spectral Confocal Microscope TCS SP2 AOBS (Leica) and a 63× oil immersion objective (HCX PL APO Oil, NA 1.32). Confocal image acquisition consisted of four images of *z*-dimension with a step size of 1 μm and image size of 0.1 μm/pixel (1024×1024). The pinhole was set at 1 Airy unit. Double-immunofluorescence staining was visualized by sequential acquisition of separate colour channels to avoid cross-talk between fluorochromes.

In order to confirm the intactness of the cells and the specificity of the Nogo-A surface staining, antibody against β-tubulin III was used with or without permeabilization (for intracellular and surface staining, respectively; described above) of cell membrane.

To confirm the confocal microscopy results, we performed pre-embedding immunoelectron microscopy using colloidal gold. Cells were quenched in 1% $NaBH_4$, blocked with IgG-free BSA (Jackson ImmunoResearch Laboratories) for 1 hour and incubated with the primary antibody (as described in the above section). Following incubation with the secondary antibody, cells were treated with 10-nm colloidal gold particles conjugated with Protein A (BBInternational) and processed for routine plastic embedding. Ultra-thin sections were analyzed with a Zeiss electron microscope EM10 and images were taken with a GATAN camera.

Intracellular staining

Dissociated DRGs plated on PLL- and laminin-coated glass coverslips and cultured for either 10 or 24 hours were washed with PBS and fixed with 4% PFA for 20 minutes. After permeabilization with 0.3% Triton X-100 and washing with PBS, cells were incubated in blocking buffer (2% goat serum, 0.2% fish skin gelatine in PBS) and subsequently with primary antibody for 30 minutes. Following 30 minutes incubation with secondary antibody, coverslips were mounted on slides with Mowiol containing 0.1% DABCO. For lower magnification imaging, cultures were imaged with an AxioCam HRm (Zeiss) camera coupled to a Zeiss Axioskop 2 equipped with a 10× objective (Plan NEOFLUAR, NA 0.3). Confocal imaging was done as described in the above section.

Immunohistochemistry

Tissue sections were permeabilized and incubated with a blocking buffer (3% donkey serum, 0.3% Triton X-100 in TBS) for 30 minutes at room temperature. Primary antibody was applied overnight at 4°C and, after

washing with TBS, sections were incubated with the secondary antibody for 2 hours at room temperature. Finally, sections were counterstained with Hoechst dye and mounted with Mowiol.

In ovo injections of anti-Nogo-A antibodies

Fertilized eggs obtained from a local hatchery were incubated at 38.5-39°C and staged according to Hamburger and Hamilton (Hamburger and Hamilton, 1951). Anti-Nogo-A antibody 11C7 (1 μl; 1.7 mg/ml) or a control antibody was injected into the limb bud three times over 36 hours. The ROCK inhibitor Y27632 was diluted in PBS and 0.04% Trypan Blue to the final concentration of 6.7 μg/ml and 1 μl was injected three times over 36 hours. Embryos were sacrificed at HH26, fixed in 4% PFA, and stained as wholemounts with an anti-neurofilament 160 antibody, as previously described (Perrin and Stoeckli, 2000).

To determine the distribution of the injected antibody, some embryos were fixed in 4% PFA 4 hours after the last injection of the 11C7 anti-Nogo-A antibody. These embryos were subsequently processed with Cy3-conjugated goat anti-mouse secondary antibody to visualize the injected 11C7 antibody.

In order to assess the specificity of our function-blocking anti-Nogo-A antibody 11C7, and to rule out the possibility of sterical shielding of unspecific epitopes, we injected several embryos with an antibody against the immunoglobulin superfamily adhesion molecule SC1 (also known as BEN) (Pourquie et al., 1990). Depletion of BEN showed no effect on fasciculation and pathfinding of motor axons in the developing chick hindlimb (Fig. 6I).

Analysis of fore- and hindlimb innervation pattern in Nogo-A KO mouse embryos

To visualize the complete set of nerves innervating the developing limbs, E12.5, E13.5 and E15.5 wild-type and Nogo-A KO mouse embryos were collected and processed for whole-mount immunohistochemistry with anti-neurofilament 160 antibody, as previously described (Maina et al., 1997).

In situ hybridization

For in situ hybridization analysis, digoxigenin (DIG)-labeled sense and antisense cRNA probes complementary to chicken and mouse Nogo-A sequences were prepared from a 316 bp-long fragment of chicken Nogo-A (bp 1343-1659) and by using the mouse Nogo-A exon three sequence (2361 bp), which encodes the main neurite outgrowth and cell spreading-inhibitory region of this protein. In situ hybridization was performed as previously described (Schaeren-Wiemers and Gerfin-Moser, 1993).

RESULTS

Neutralization or genetic ablation of Nogo-A enhances neurite outgrowth and fasciculation in DRG explant cultures

To assess the role of Nogo-A in developing neurons, we analyzed the neurite outgrowth of neonatal mouse and rat DRG explants in the presence of function-blocking, monospecific anti-Nogo-A monoclonal antibodies (11C7 or 7B12) or a control antibody. The neurite outgrowth pattern was analyzed by determining the average length of the 10 longest neurites per DRG, defasciculation points were counted at a distance of 300 μm from the DRG, and the percentage of thin (0.4–1.2 μm), intermediate (1.3–4 μm), and thick (4.1–15 μm) neurite fascicles that emerged from the ganglion surface was determined (Rutishauser et al., 1978).

The presence of either 11C7 or 7B12 anti-Nogo-A antibody in the medium of DRG explant cultures (5-7 days in vitro) resulted in a dramatic change in the morphology and the diameter of the neurite halo (Fig. 1A). Anti-Nogo-A antibody treatment doubled the length of radial outgrowth (Fig. 1B) and led to a reduction in the number of defasciculation points at 300 μm from DRG edges (Fig. 1C). A marked shift from predominantly thin to thick fascicles extending from DRGs was observed in the presence of either the 11C7 or the 7B12 anti-Nogo-A antibody (Fig. 1D).

The effects of anti-Nogo-A antibodies on neurite outgrowth and morphology were dose dependent with maximal results obtained with an antibody concentration of 10 μg/ml (see Table S1 in the supplementary material). One third of this concentration still produced a detectable shift from thin to thick fascicles, but higher amounts of antibodies did not increase the differences in neurite morphology (see Table S1 in the supplementary material). When these function-blocking anti-Nogo-A antibodies were applied in neonatal rat DRG explant cultures, very similar results to the ones shown here for mouse DRGs were obtained (data not shown).

To investigate the possibility that ganglia from different parts of the spinal column vary in their response to anti-Nogo-A antibodies, cervical, thoracic and lumbar DRGs from newborn mice were cultured in medium containing either control or anti-Nogo-A antibodies (11C7 or 7B12). The effects of Nogo-A neutralizing antibodies on the length and fasciculation of neurites emanating from the DRG explants were comparable for all the spinal levels (see Table S2 in the supplementary material).

As an alternative to acute ablation of Nogo-A by function-blocking anti-Nogo-A antibodies, we used DRGs from neonatal Nogo-A KO mice. The pattern of neurites growing out from Nogo-A KO DRGs was strikingly different from that of wild-type DRGs, but very similar to that of DRGs treated with anti-Nogo-A antibodies (Fig. 1A): a two-fold increase in the length of radial outgrowth compared with wild-type DRG explants (Fig. 1B); a severely reduced number of defasciculation points (Fig. 1C); and an increased fraction of thick fascicles emanating from the ganglia (Fig. 1D).

In order to confirm that the effects of function-blocking anti-Nogo-A antibodies 11C7 and 7B12 on neurite outgrowth from wild-type DRGs were specific, we applied the antibodies to cultures of Nogo-A KO DRGs. The measured parameters were indistinguishable from those seen in non-treated Nogo-A KO DRG cultures (Fig. 1B-D), thus confirming the specificity of the anti-Nogo-A antibody effects. In western blots, both monoclonal anti-Nogo-A antibodies recognized a single band corresponding to Nogo-A at a molecular mass of ~190 kDa (see Fig. S1A in the supplementary material).

Scanning and transmission electron microscopy (TEM) observations confirmed the effects of function-blocking anti-Nogo-A antibodies on DRG neurites: straight, thick fascicles with a reduced ability to defasciculate from each other, rather than networks of fine, interlaced processes, were consistently seen when the function of Nogo-A was blocked (Fig. 2A,B). As shown in Fig. 2C,D, treatment of wild-type DRGs with the anti-Nogo-A antibody 11C7 caused a marked increase in the average number of neurites per fibre bundle when compared with the control antibody-treated cultures.

Neutralization of Nogo-A alters branching and elongation of dissociated DRG neurons

In order to investigate whether Nogo-A plays a role in neurite elongation and branching of single cells, we cultured dissociated DRG neurons from wild-type neonatal mice for 10-24 hours in the presence of either 11C7 or 7B12 Nogo-A neutralizing antibodies. Length of the longest neurite, total neurite length, rectilinearity of neurites, length of the primary neurites before the first branch point, number of primary neurites per neuron, number of branch points per neuron, and the size of branch angles between the daughter and parent neurite were quantified.

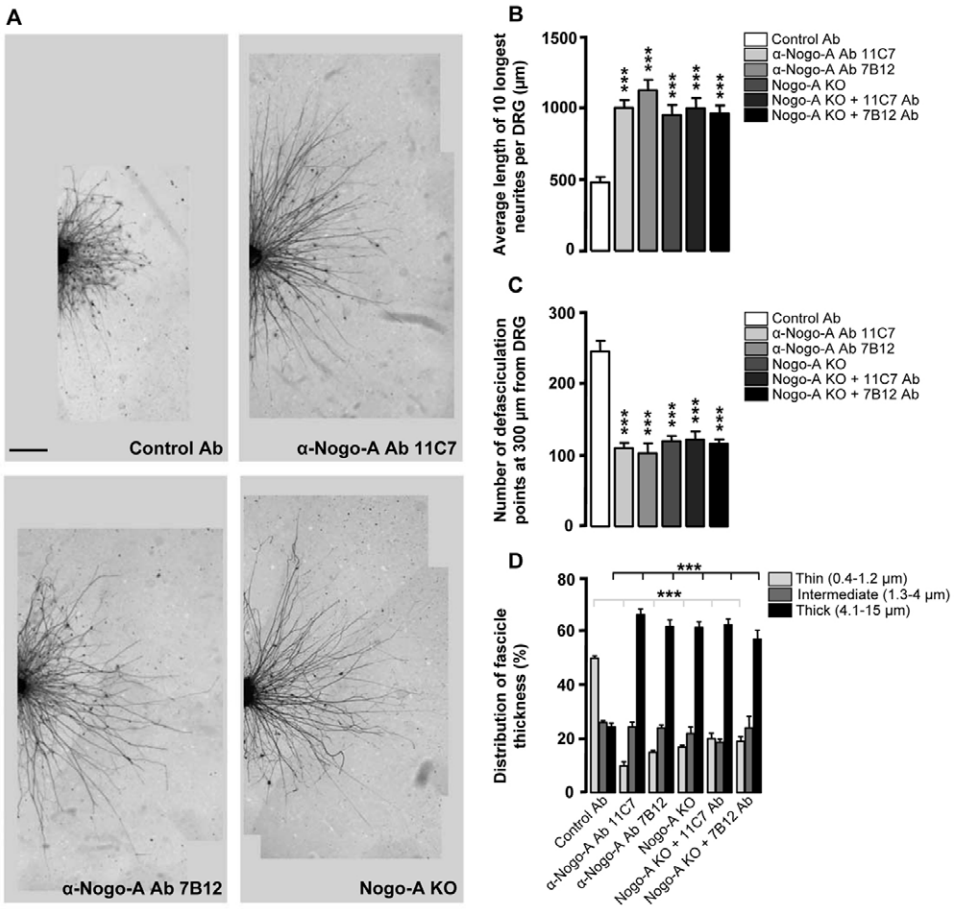

Fig. 1. Neutralization of Nogo-A by anti-Nogo-A antibodies or by genetic ablation leads to an increase in the length and fasciculation of neurites in DRG explant cultures. (**A**) DRG explants dissected from neonatal wild-type (Control Ab) or Nogo-A KO mice were cultured in the presence of either control or anti-Nogo-A (11C7 or 7B12) antibodies, or without any treatment. Inactivation of Nogo-A resulted in the outgrowth of longer, straighter and thicker neurites, instead of the tangled net of fine processes formed in the control antibody-treated cultures. Scale bar: 300 μm. (**B**) Inactivation of Nogo-A, either by function-blocking antibodies or by genetic ablation results in an increased radial outgrowth length from DRG explants. Antibodies had no effect on Nogo-A KO neurons. (**C**) The number of defasciculation points was decreased in Nogo-A KO or anti-Nogo-A antibody-treated wild-type DRGs. (**D**) Nogo-A neutralization or knockout increased the percentage of thick bundles emanating from the DRGs. Control antibody-treated wild-type DRGs did not differ significantly from non-treated ones (data not shown) and therefore are shown as controls. Values represent means ± s.e.m. of 39-59 ganglia per condition from four independent experiments; ***P<0.0001, Student's t-test.

Upon neutralization of Nogo-A, dissociated DRG neurons sent out significantly longer individual neurites than when treated with control antibody (Fig. 3A,B). In addition, these neurites appeared to be straighter than the control antibody-treated ones (Fig. 3A). The rectilinearity index [the ratio between the length of a straight line between the origin and the distal end of the neurite and its actual length (Bouquet et al., 2004)] showed that neurites of anti-Nogo-A antibody-treated cells were much straighter (11C7, 0.937±0.0198, n=89; 7B12, 0.942±0.031, n=83) than the control antibody-treated neurons, which exhibited a more wavy growth (0.787±0.0287, n=82; P<0.001).

Interestingly, the sum of the length of all neurites per neuron was almost identical among all treated groups (Fig. 3C), as was the number of primary neurites (control antibody, 3.63±0.17, n=82; 11C7, 3.59±0.21, n=89; 7B12, 3.78±0.18, n=83). The increased length of individual neurites was therefore mainly due to the reduction in branching, which was observed as a decrease in the number of branch points per neuron in the anti-Nogo-A antibody-treated cultures (Fig. 3D). In addition, the presence of anti-Nogo-A antibodies caused the first branch points to occur further away from the cell body than in control antibody-treated cultures (control antibody, 10.79±1.14 μm, n=82; 11C7, 23.42±1.914 μm, n=89; 7B12, 25.38±2.324 μm, n=83; P<0.0001).

We also measured the angles formed by the branches with their neurites of origin. Collateral branches usually form at almost right angles (90°) from the parent neurite (Kalil et al., 2000). In control antibody-treated cultures, ~60% of the branches formed at an angle of 81-90°; smaller angles of 40-80° were rare (~15% of branches; Fig. 3E). In anti-Nogo-A antibody-treated neurons, the frequency of 81-90° angles decreased to ~42%, whereas the fraction of small angle branches increased to ~30% compared with control antibody-treated cells (Fig. 3E). These results suggest a reduction in the repulsive interactions between neurites after neutralization of Nogo-A.

Similar observations were made in cultures of dissociated Nogo-A KO DRG neurons (Fig. 3A). Genetic ablation of Nogo-A resulted in an increased length of the longest neurite (Fig. 3B), but did not change the sum of neurite length per cell when compared with that of wild-type cells (Fig. 3C). The rectilinearity index was higher in Nogo-A KO DRG neurons than in wild-type controls (0.926±0.0198, n=81 versus 0.787±0.0287, n=82; P<0.001), thus confirming that the lack of Nogo-A leads to straighter neurite trajectories (Fig. 3A). Nogo-A KO cells had significantly fewer branch points per neuron than control cells (Fig. 3D), whereas the number of primary neurites emanating from the cell body did not show a significant difference (wild type, 3.63±0.17, n=82; Nogo-A KO, 3.68±0.16, n=81). The length of the unbranched primary neurites was increased in Nogo-A KO cells compared with in wild-type controls (wild type, 10.79±1.14 μm, n=82; Nogo-A KO, 24.00±2.36 μm, n=81; P<0.0001). The percentage of branches formed at large angles (81-90°) decreased in Nogo-A KO DRG neurons from ~60% to ~44%, whereas the proportion of small angle branches (40-80°) increased from ~17% to ~33% (Fig. 3E). When anti-Nogo-A antibodies were added to cultures of Nogo-A KO neurons, no additional effects were seen (Fig. 3B-E).

The specificity of these effects with regard to Nogo-A was supported by rescue experiments in which Nogo-A KO DRG neurons were transfected with adeno-associated viruses (AAV)

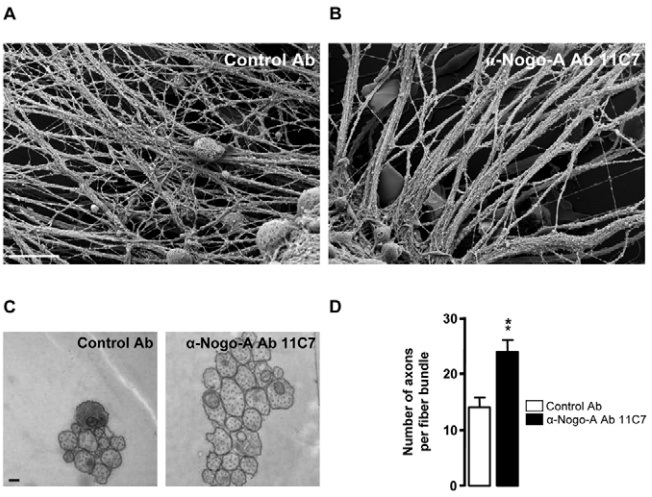

Fig. 2. Neurite outgrowth from wild-type neonatal mouse and rat spinal ganglia is highly fasciculated in the presence of anti-Nogo-A antibody 11C7. (**A**,**B**) Scanning electron micrographs of neurite outgrowth from newborn mouse lumbar DRGs. Control antibody-treated DRG cultures show a typical, highly interlaced network of fine neurites (A), whereas thick, well-spaced neurite bundles were formed in the presence of anti-Nogo-A antibody 11C7 (B). Scale bar: 10 μm. (**C**) Ultrastructural analysis of cross-sectioned neurite bundles. Scale bar: 0.2 μm. (**D**) Anti-Nogo-A antibody treatment increases the number of neurites per fibre bundle. Values represent means ± s.e.m. of 21-23 fibre bundles per condition from three independent experiments; ***P*<0.001, Student's *t*-test.

serotype 2 (AAV2) expressing either green fluorescent protein (eGFP) or Nogo-A (see Fig. S2A,B in the supplementary material). Expression of Nogo-A rescued the Nogo-A KO phenotype: the length of the longest neurite was decreased towards wild-type values (see Fig. S2C in the supplementary material); the number of branch points was increased (see Fig. S2E in the supplementary material); and the rectilinearity index was lower in AAV2.Nogo-A expressing neurons than in the plain Nogo-A KO ones (0.796±0.0294, *n*=89 versus 0.932±0.0193, *n*=86, respectively; *P*<0.001). The length of the unbranched primary neurites was decreased in Nogo-A KO cells treated with AAV2.Nogo-A compared with in AAV2.eGFP-treated controls (Nogo-A KO+AAV2.Nogo-A, 11.23±1.19 μm, *n*=89; Nogo-A KO+AAV2.eGFP, 22.93±2.41 μm, *n*=86; *P*<0.0001). The percentage of branches formed at large angles (81-90°) increased after expression of Nogo-A in Nogo-A KO DRG neurons from ~45% to ~58%, whereas the proportion of small angle branches (40-80°) decreased from ~36% to ~20% (see Fig. S2F in the supplementary material).

As the experiments with dissociated DRG neurons suggested a cell-autonomous effect, we prepared mixed cultures of wild-type and Nogo-A KO DRG neurons in order to assess whether, upon contact, they can affect the phenotype of one another. As shown in Fig. S3A in the supplementary material, cell bodies of wild-type and Nogo-A KO neurons did not associate with each other, but rather made frequent contact with the cell of the same genotype (see Fig. S3B,C in the supplementary material). In these cultures ~54% of cells were forming 'doublets' (two cell bodies touching each other), ~32% were single cells, and ~14% of the cells were making contacts with multiple cells. Because we could not assess the phenotype of each cell in multi-cell conglomerates, we focused on the 'doublets'. Of all the doublets, ~57% were made by Nogo-

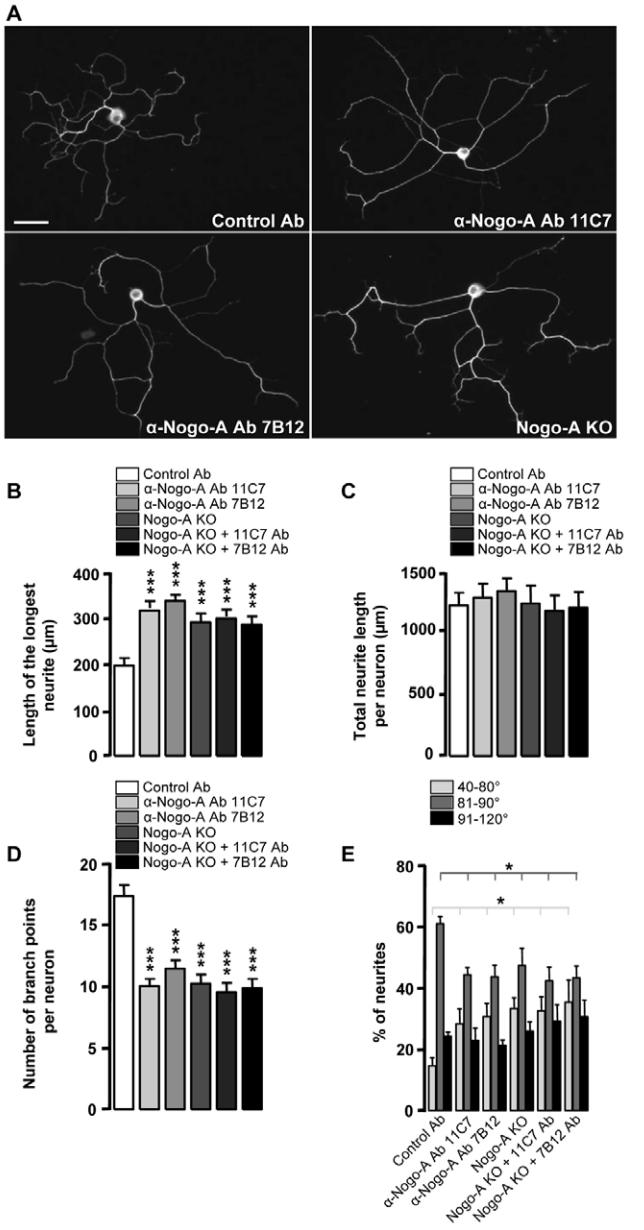

Fig. 3. Neutralization of Nogo-A leads to increased length and reduced branching of DRG neurites. (**A**) Dissociated DRGs from neonatal wild-type (Control Ab) or Nogo-A KO mice were cultured for 10-24 hours in the presence of either control or anti-Nogo-A (11C7 or 7B12) antibodies, or without any treatment. Neutralization of Nogo-A resulted in the outgrowth of longer and straighter neurites with a reduced number of branches. Scale bar: 50 μm. (**B**) Downregulation of Nogo-A by either anti-Nogo-A antibodies or genetic ablation (Nogo-A KO) resulted in an increased length of the longest neurites emanating from the DRG neurons. (**C**) The total length of all neurites per neuron was not affected by the absence of Nogo-A. (**D**) The number of branch points per neuron was markedly reduced when Nogo-A was inactivated. (**E**) Quantitation of the angles between the daughter and parent neurite showed that the deletion of Nogo-A leads to a decrease in the percentage of neurites forming branches at large (81-90°) angles, and an increase in the proportion of neurites branching off at small angles (40-80°). Control antibody-treated wild-type DRGs did not differ significantly from non-treated ones (data not shown) and therefore are shown as controls. Values represent means ± s.e.m. of 81-89 neurons per condition from four independent experiments; **P*<0.05 and ****P*<0.0001, Student's *t*-test.

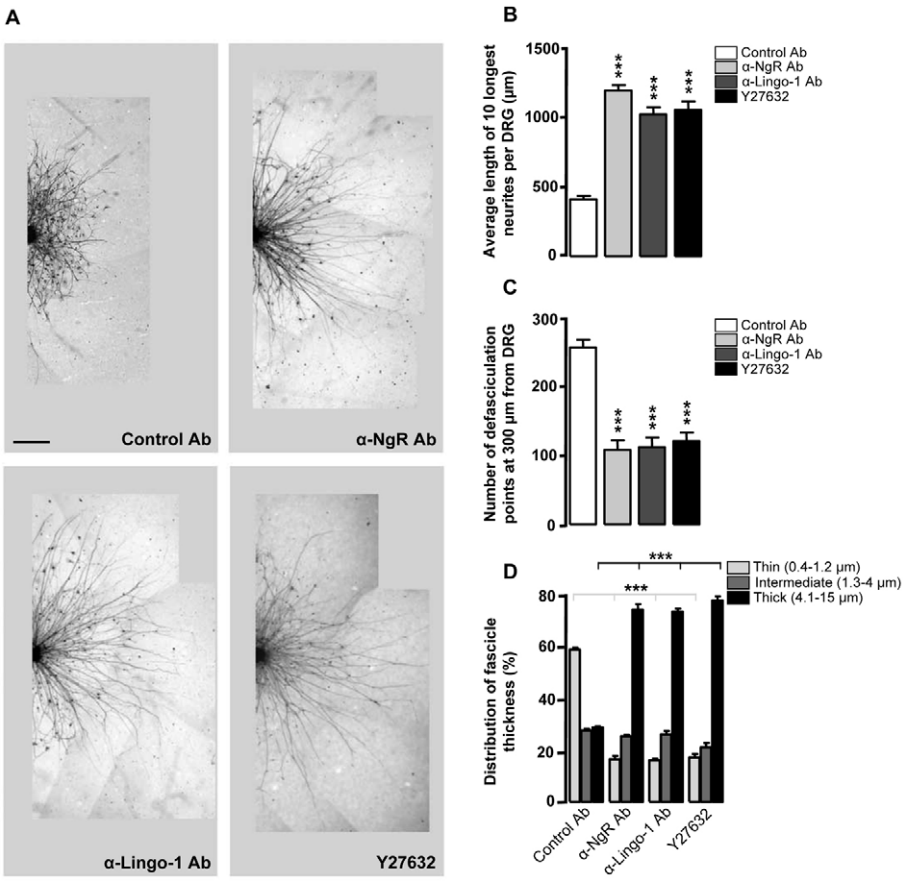

Fig. 4. Antibodies against NgR or Lingo1, or ROCK blockade lead to increased length and fasciculation of neurites in DRG explant cultures. (**A**) Lumbar DRGs explanted from wild-type newborn mice were cultured for 5-7 days in the presence of either anti-NgR or anti-Lingo1 antibodies, or with the ROCK inhibitor Y27632. The presence of any of these resulted in the formation of long, straight and thick fibre bundles instead of the interlaced network of fine processes formed in control cultures. Scale bar: 300 μm. (**B-D**) Antibodies against NgR or Lingo1, or the blockade of ROCK resulted in an increased length of radial outgrowth (B), a reduced number of defasciculation points at 300 μm from the ganglia (C), and thicker neurite bundles growing out of the DRGs (D). Values represent means ± s.e.m. of 48–59 ganglia per condition from four independent experiments; ***P<0.0001, Student's t-test.

A KO cells and 43% were formed by wild-type DRG neurons. Mixed wild-type–Nogo-A KO doublets were not observed, which suggests there are differences in adhesion/repulsion between the two cell types.

Cultures of dissociated DRG neurons were used to verify the presence of Nogo-A on the cell surface. Immunostaining of dissociated, live neonatal mouse DRG neurons with a polyclonal, monospecific rabbit antibody recognizing the Nogo-A specific region [Rb173A/Laura (Dodd et al., 2005; Oertle et al., 2003)] demonstrated punctate distribution of Nogo-A on the surface of neuronal cell bodies and their processes (see Fig. S4B in the supplementary material). The presence of Nogo-A on the cell surface was further confirmed by immunogold electron microscopy (see Fig. S4E in the supplementary material). Nogo-A staining was completely absent on neurons of Nogo-A KO mice (see Fig. S4C,F in the supplementary material). Additionally, *NgR* mRNA was clearly present in DRG neurons from E15 to P60 (see Fig. S4G in the supplementary material). Western blots confirmed the expression of NgR protein in both wild-type and Nogo-A KO DRG neurons at E15 (see Fig. S4H in the supplementary material).

Antibodies against NgR or Lingo1, or blockade of ROCK signalling, increases neurite fasciculation and decreases branching of DRG neurons

Nogo-A has been shown to cause neurite growth inhibition and growth cone collapse via a receptor complex including NgR, p75/TROY and Lingo1 (Bandtlow and Dechant, 2004; Fournier et al., 2001; Mi et al., 2004). Blockade of these components, or of downstream Rho-A/ROCK activation, allows neurite outgrowth on Nogo-A-containing substrates both in vitro and in vivo (Schwab, 2004; Yiu and He, 2006). When we applied antibodies against NgR or Lingo1 to neonatal mouse DRG explants, neurites were longer and were organized in well-spaced bundles with straight trajectories (Fig. 4A,B). Additionally, a decrease in the number of defasciculation points counted at 300 μm from the DRG (Fig. 4C) and a higher proportion of thick (4.1-15 μm) fascicles (Fig. 4D) were observed in these cultures. Inactivation of ROCK by Y27632 mimicked the results obtained following neutralization of its upstream signalling partners, Nogo-A, NgR and Lingo1 (Fig. 4A), and led to an increased length of radial outgrowth (Fig. 4B), a twofold decrease in the number of defasciculation points at 300 μm from the DRGs (Fig. 4C), and an increase in the proportion of thick fibre bundles growing out from the DRG (Fig. 4D). Almost identical results as shown here for mouse DRGs were seen when newborn rat DRG explants were used (data not shown).

The addition of anti-NgR, anti-Lingo1 or the ROCK blocker Y27632 to cultures of dissociated DRG neurons induced very similar changes to those observed after neutralization or genetic ablation of Nogo-A (compare Fig. 3A with Fig. 5A): an increased length of the longest neurite per cell (Fig. 5B), and a decreased number of branches (Fig. 5D). The total neurite length per cell did not significantly differ between the groups (Fig. 5C) and the number of primary neurites per cell was not significantly changed (control antibody, 3.81±0.18, n=87; anti-NgR, 3.74±0.16, n=92; anti-Lingo1, 3.78±0.18, n=89; Y27632, 3.69±0.19, n=94). The rectilinearity index was higher for neurons grown in presence of anti-NgR or anti-Lingo1 antibodies or with Y27632 (control

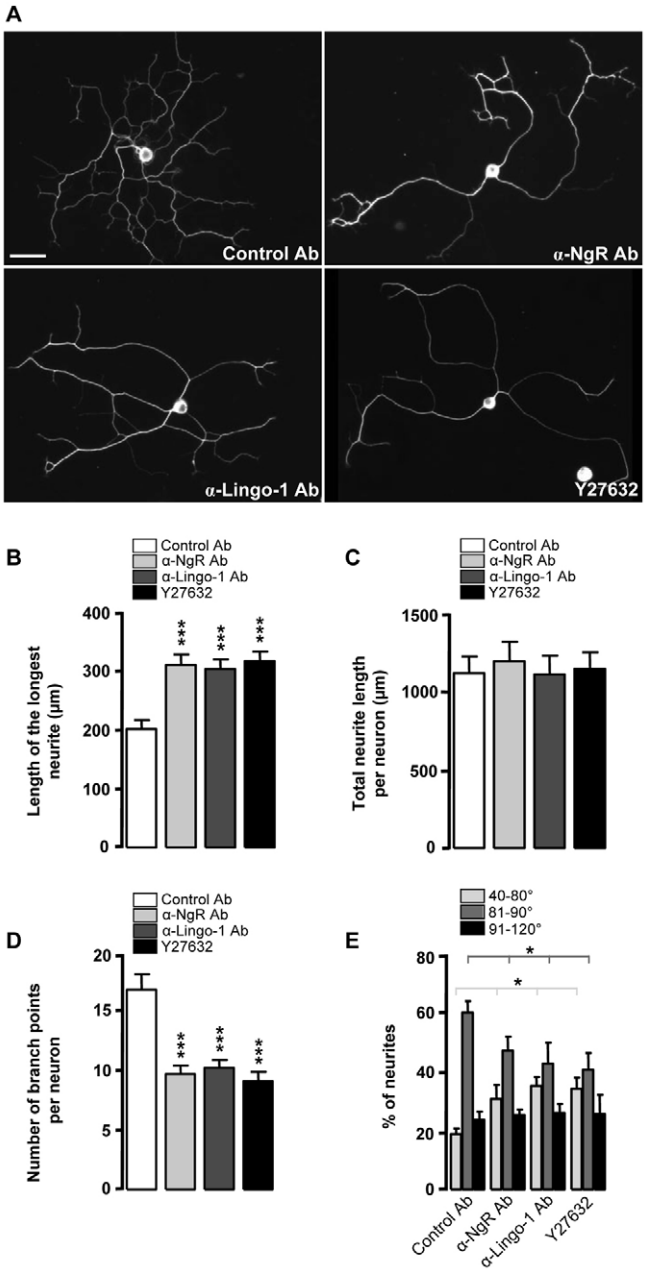

Fig. 5. Antibodies against NgR or Lingo1, or ROCK blockade lead to increased neurite length and decreased branch formation in dissociated DRG neurons. (**A**) Dissociated DRGs of wild-type neonatal mice were cultured for 10-24 hours in the presence of either control or anti-NgR or anti-Lingo1 antibody. Length and straightness of DRG neurites were increased, whereas their branching was reduced. The same results were observed after Y27632 blockade of ROCK. Scale bar: 50 μm. (**B**) Length of the longest neurite emanating from the DRG neurons was increased after application of anti-NgR or anti-Lingo1 antibodies. The same results were observed after Y27632 blockade of ROCK. (**C**) The total length of all neurites of a given neuron was not altered in the presence of either anti-NgR or anti-Lingo1 antibodies, or after Y27632 blockade of ROCK activity. (**D**) Antibodies against NgR or Lingo1, or Y27632 blockade of ROCK activity lead to a decreased number of branch points per neuron. (**E**) Branches had smaller angles with their parental neurites after application of anti-NgR or anti-Lingo1 antibodies. The same results were observed after Y27632 blockade of ROCK. Values represent means ± s.e.m. of 87-94 neurons per condition from four independent experiments; **P*<0.05 and ****P*<0.0001, Student's *t*-test.

antibody, 0.796±0.0198, *n*=87; anti-NgR, 0.938±0.0228, *n*=92; anti-Lingo1, 0.919±0.0186, *n*=89; Y27632, 0.912±0.0139, *n*=94; *P*<0.001), and primary neurites sent out first branches further away from the cell body than did the cells in control antibody-treated cultures (control antibody, 10.74±0.8913 μm, *n*=87; anti-NgR, 25.79±2.271 μm, *n*=92; anti-Lingo1, 21.64±2.113 μm, *n*=89; Y24632, 23.72±2.869 μm, *n*=94; *P*<0.0001). The number of branches formed at large angles (81-90°) decreased and proportion of branches formed at small angles (40-80°) from the parent branch increased (Fig. 5E), thus pointing to a reduction in repulsive forces between neurites.

On western blots of mouse brain lysates, a single band of ~51 kDa corresponding to NgR was detected by the anti-NgR antibody (see Fig. S1B in the supplementary material). The antibody against Lingo1 detected the full length Lingo1 protein at ~83 kDa, as well as fragments at ~17 and ~34 kDa, which correspond to known cleavage and degradation products (as stated by the manufacturer; see Fig. S1C in the supplementary material).

Neutralization of neuronal Nogo-A leads to progressive adhesion and neurite fasciculation

Time-lapse imaging was used to evaluate the sequence of events leading to bundle formation upon neutralization of Nogo-A on the surface of DRG neurons.

In the first set of experiments, we made time-lapse movies of neurites growing out from Nogo-A KO or wild-type DRGs treated either with control or 11C7 Nogo-A neutralizing antibody, which was added at the time of plating. Neutralization of Nogo-A either by function-blocking antibodies or by genetic ablation resulted in highly bundled, straight neurites growing out of the explants, as opposed to the highly dynamic plexus of fine, intermingled neurites that appeared when DRG explants were treated with the control antibody (see Movies 1-3 in the supplementary material). The tips of the bundles advanced rapidly; bundle formation seemed to increase over time (see Movies 2, 3 in the supplementary material). Quantification of fasciculation revealed a significantly reduced number of neurites and bundles at the distance of 150 μm from the DRG when Nogo-A was neutralized or genetically ablated (wild type+control antibody, 55.00±3.027, *n*=18; 11C7, 37.33±3.177, *n*=20; Nogo-A KO, 34.71±3.283, *n*=19; *P*<0.0001).

In the second set of time-lapse experiments, we investigated whether delayed addition of an anti-Nogo-A antibody can cause a shift from smaller to larger fascicles. We imaged wild-type non-treated DRGs for 5 hours before the anti-Nogo-A antibody 11C7 was added. During that time, a complex plexus of thin, interlaced neurites was formed (see Movie 4 in the supplementary material). Soon after the addition of the 11C7 antibody, the plexus started to disappear, turning into bundles of straight neurites (see Movie 4 in the supplementary material). This movie also shows that the transformation was caused mainly by neurites adhering to each other laterally, thus progressively assembling into thicker fascicles. By the end of the imaging period, 15 hours after addition of the antibody, most of the neurites had assembled into bundles and the highly elaborated neurite plexus was significantly reduced (see Movie 4 in the supplementary material). This increase in fasciculation was confirmed by the reduction in the number of processes/fascicles quantified at a distance of 150 μm from the DRGs following the neutralization of Nogo-A on the surface of neurites with 11C7 antibody (wild type, 58.10±3.459, *n*=21; 11C7, 34.86±3.192, *n*=18; *P*<0.0001).

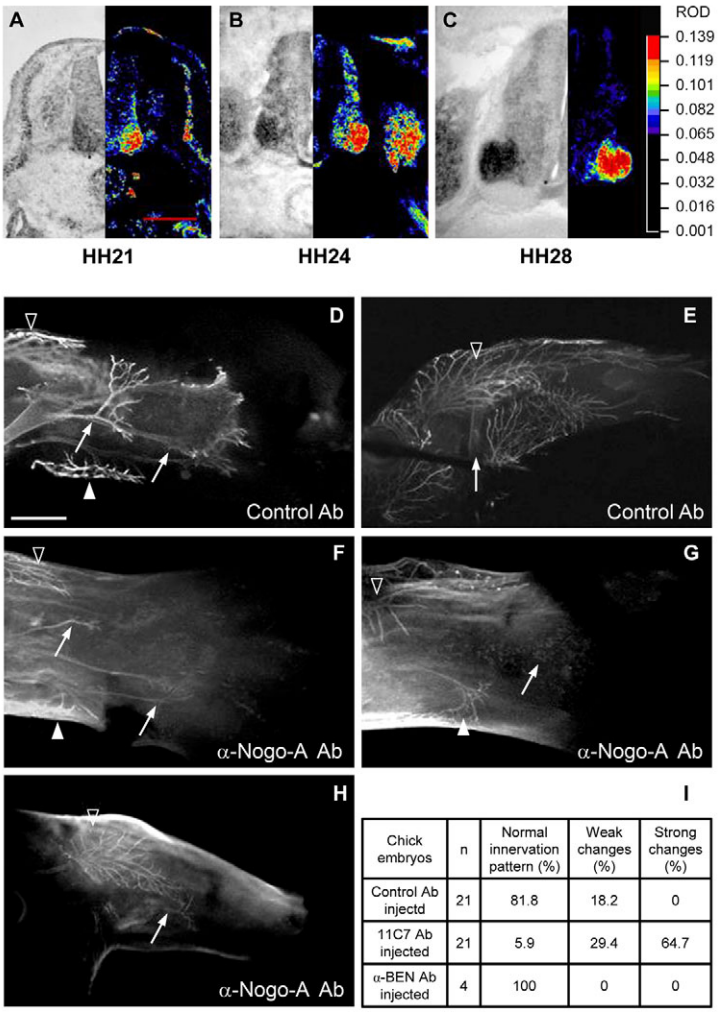

Chick embryos	n	Normal innervation pattern (%)	Weak changes (%)	Strong changes (%)
Control Ab injectd	21	81.8	18.2	0
11C7 Ab injected	21	5.9	29.4	64.7
α-BEN Ab injected	4	100	0	0

Fig. 6. Neutralization of Nogo-A interferes with peripheral nerve formation in the developing chicken embryo hindlimb. (**A-C**) Localization of *Nogo-A* mRNA during spinal cord development. In situ hybridization reveals *Nogo-A* expression in motoneurons and dorsal root ganglia at the lumbosacral spinal cord during the time of axon outgrowth at HH21. *Nogo-A* continues to be expressed during pathfinding and muscle innervation at HH24 and HH28. Importantly, *Nogo-A* mRNA is absent from the ventral roots, indicating that Schwann cells do not express Nogo-A. ROD, relative optical density. Scale bar: 200 μm. (**D-H**) Dorsal (D,F,G) and anterior (E,H) views of the limb bud are shown. Peripheral axons fail to correctly innervate the distal limb in the absence of Nogo-A. In limb buds injected with the anti-Nogo-A antibody 11C7, axons mostly failed to leave the plexus area (F-H). In aged-matched control limb buds that were injected with a control antibody (D,E), axons formed the characteristic nerve trunks found in non-treated control embryos (not shown). The sciatic nerve was severely affected (arrows); in many embryos the nerve was not formed at all (arrows in F). Fibres formed nerve bundles that extended along aberrant pathways and often failed to reach the distal part of the limb (arrow in G). White arrowhead in F and G indicates a nerve extending along the posterior margin of the limb bud that was less strongly affected in anti-NogoA antibody-treated embryos, compare with white arrowhead in D. The open arrowhead indicates the most anterior nerve of the limb bud that normally branches extensively and straddles the anterior edge of the limb bud by extending both dorsally and ventrally, as seen in D,E. Scale bar: 500 μm. (**I**) Hindlimb innervation patterns were classified into three groups: no defect, weak abnormalities (distal nerves were disorganized but could clearly be identified), and severe changes in the innervation pattern, including the absence of distal nerves.

Neutralization of Nogo-A in chicken embryos results in aberrant peripheral nerve formation

The developing chick peripheral nervous system has served as an excellent model system for studies of axon-axon interactions during peripheral nerve formation and axonal pathfinding (Rafuse and Landmesser, 2000; Tang et al., 1992; Tang et al., 1994). Therefore, we turned to this experimental model to investigate the influence of Nogo-A on peripheral fibre growth and branch formation in vivo.

Between stages 21 and 26 (HH21-26) (Hamburger and Hamilton, 1951), i.e. during the time window of initial hindlimb innervation, *Nogo-A* mRNA is expressed in both motor and sensory neurons (Fig. 6A-C). Their axons reach the lumbar plexus at HH21; they then go through a waiting period before they sort out to select either a dorsal or a ventral pathway through the limb bud (Wang and Scott, 2000). At HH23, they resume growth and extend distally into the limb bud.

We injected the function-blocking anti-Nogo-A antibody 11C7 into the limb buds of chicken embryos in ovo. Injections started at HH18, i.e. when motor and sensory axons leave the spinal cord and the DRG respectively, but before they reach the plexus region. Injections of 1.7 μg of antibody were repeated every 12 hours until the embryos were sacrificed at HH26. This approach was previously used to analyze the effect of CAMs on hindlimb innervation and has the advantage that the functional blockade can be targeted to the region of interest and at the desired developmental stages (Landmesser et al., 1988; Tang et al., 1994). Western blot analysis of embryonic chicken HH24 brain lysates showed that in chick the 11C7 antibody also recognizes a single band of ~190 kDa, which corresponds to Nogo-A (see Fig. S1A in the supplementary material). Immunofluorescence at 4 hours after the antibody injection showed a distribution over the entire limb, with minimal diffusion into the contralateral limb (see Fig. S5 in the supplementary material).

Injection of the 11C7 antibody resulted in the failure of axons to innervate the distal hindlimb correctly (Fig. 6D-H). Axons reached the plexus, but often failed to sort out and leave the plexus area (Fig. 6F-H). In some embryos, axons did not reach the distal part of the hindlimb (Fig. 6G). The few axons that succeeded to extend into the distal limb grew along aberrant pathways (Fig. 6F-H) instead of choosing the appropriate dorsal or ventral trajectory to reach the respective muscle mass. Neutralization of Nogo-A also led to a dramatic decrease in branch formation of the nerves (Fig. 6, compare D,E with F-H).

For quantitative assessment the hindlimb innervation patterns were grouped into three classes by two independent blinded observers: normal innervation pattern, weak changes (some pathfinding errors, but the innervation pattern was mainly normal), or strong changes (only very few fibres present in the distal limb bud; neither the crural nor the sciatic nerves were formed). Results confirmed a highly aberrant hindlimb innervation in the anti-Nogo-A antibody-injected embryos (Fig. 6I).

We used the same approach to block the downstream effector ROCK by repeated injections of Y27632. The effects on axonal branching and sorting in the plexus region were less severe than after blockage of Nogo-A function (see Fig. S6A-C in the supplementary material). However, this might be explained by the suboptimal concentration of the ROCK inhibitor in the embryo; injection of 20 ng was lethal, and, even after injections of 3.35 ng three times between HH18 and HH26, survival was decreased compared with that of control embryos injected with PBS.

Nogo-A KO mouse embryos show increased fasciculation and decreased branching of nerves innervating fore- and hindlimbs

During the time of fore- and hindlimb innervation, between E10.5 and E15.5, *Nogo-A* mRNA was expressed both by motoneurons in the spinal cord and sensory neurons in the DRGs (Fig. 7A). Levels of *Nogo-A* mRNA increased in motoneurons and DRGs until embryonic day 15.5 (Fig. 7A), i.e. during the time when axons defasciculate in muscles and skin to form their stereotypical branching patterns. Immunohistochemistry was consistent with the in situ hybridization data (see Fig. S7 in the supplementary material): motor and sensory axons stained intensely for Nogo-A during the period when they grow from the plexus region into the limb to form the major nerve trunks and muscle nerves (E11.5-E13.5; see Fig. S7 in the supplementary material). Mesenchymal cells and early forming myotubes were also Nogo-A positive, but staining was clearly weaker than that seen in the nerves (see Fig. S7 in the supplementary material).

We analyzed fore- and hindlimb innervation in wild-type and Nogo-A KO embryos (E12.5-E13.5) by whole-mount immunohistochemistry using an antibody against neurofilament 160.

Development of forelimb innervation

The median nerve, which innervates the palmar side of the hand, starts to branch extensively at E12.5 in wild-type embryos (Fig. 7B). Forelimb innervation and its analysis are schematically represented in Fig. S8A in the supplementary material. Quantification showed that the length of the median nerve arbour, starting from the hand paddle, was not affected in Nogo-A KO embryos, whereas its width was decreased (Fig. 7D). The dorsal side of the hand is innervated by the radial and ulnar nerve (see Fig. S8A in the supplementary material). The thickness of both nerves was increased in the Nogo-A KO embryos (Fig. 7D). The length of the ulnar nerve was not altered in the absence of Nogo-A (wild type, 249.3±12.67 μm, n=12; Nogo-A KO, 238.1±11.628 μm, n=12). Reductions in the branching pattern of both median and ulnar nerve were apparent in Nogo-A KO embryos (Fig. 7B). At E12.5, both major and fine nerve branches were missing in Nogo-A KO mice. At E13.5, the median nerve grows distally and the digital nerves form. At this developmental stage many smaller nerve branches were missing in Nogo-A KO mice (number of branches: wild type, 25.126±3.988, n=12; Nogo-A KO, 15.866±2.344, n=12; P=0.0421). The superficial network of cutaneous sensory nerves was markedly reduced in Nogo-A mutants (Fig. 7B). Such major, obvious alterations in the forelimb peripheral nerve formation were readily detectable in seven out of 12 Nogo-A KO mouse embryos.

Development of hindlimb innervation

Distal hindlimb peripheral nerve development was significantly affected by genetic inactivation of Nogo-A. At E12.5, Nogo-A KO embryos showed a significantly increased width of the sciatic nerve when compared with wild-type values (Fig. 7C,E). The deep peroneal nerve extended an average 200 μm past its branch point in both genotypes (Fig. 7E). Its width was more than doubled in Nogo-A KO embryos (Fig. 7C,E). The superficial peroneal nerve length was not significantly altered in the absence of Nogo-A (Fig. 7E), whereas the number of its branches was reduced (Fig. 7C).

At the same developmental stage, the tibial nerve width was increased in Nogo-A KO embryos (Fig. 7E) compared with in wild-type embryos. Its arbour length was similar between the two genotypes, but the arbour width and its complexity were significantly decreased in the Nogo-A KO embryos (Fig. 7E). At E13.5, the tibial nerve subdivides proximally into two major nerve trunks and distally into five branches to innervate the plantar muscles of the toes (see Fig. S8B in the supplementary material). In Nogo-A KO embryos, bifurcation of the nerve into the two major branches was disrupted (Fig. 7C) and its branching was markedly reduced (number of branches: wild type, 28.736±4.638, n=12; Nogo-A KO, 17.664±3.254, n=12; P=0.0375). The tibial nerve terminal arbour in Nogo-A KO animals appeared to be more sparsely populated with nerve branches than in wild-type littermates, suggesting that some constituents of the tibial nerve were missing (Fig. 7C). The penetrance of this phenotype was incomplete; changes in the development of the hindlimb peripheral nerves were observed in eight out of 12 Nogo-A KO embryos.

These results, together with those obtained from the chick experiments, demonstrate that perturbation of Nogo-A function produces characteristic changes in peripheral nerve formation, thickness and branching.

DISCUSSION

The inactivation of Nogo-A by gene ablation or by function-blocking antibodies in cultured DRGs led to an increased length of outgrowing neurites, a decrease in branch formation, and an increase in fasciculation of neurites. Very similar results were obtained when DRGs were treated with antibodies against NgR or Lingo1, or with the ROCK blocker Y27632. Acute in ovo neutralization of Nogo-A in the developing hindlimb of chicken embryos led to the failure of many axons to leave the sciatic plexus, increased fasciculation and an absence of major nerve branches. In Nogo-A KO mouse embryos, ablation of Nogo-A likewise caused increased fasciculation and reduced branching of peripheral nerves. Taken together, these results suggest an important role for Nogo-A in peripheral nervous system development.

Nogo-A was purified and characterized as the first CNS myelin neurite growth inhibitory protein and was shown to be present on the cell surface (in addition to a large intracellular pool) with its N-terminal, Nogo-A-specific region facing the extracellular space (Caroni and Schwab, 1988; Chen et al., 2000; Dodd et al., 2005; Huber et al., 2002; Oertle et al., 2003). Surprisingly, Nogo-A was also found in neurons, where its levels are high during development but lower or undetectable in the adult nervous system, except for in regions with a high morphological and physiological plasticity (Huber et al., 2002; Hunt et al., 2003; Josephson et al., 2001; Wang et al., 2002). Signalling via a receptor complex containing NgR, Lingo1, p75/TROY and possibly PirB, Nogo-A activates Rho-A and ROCK and participates in rearrangements of the actin cytoskeleton of the growth cone, resulting in neurite outgrowth inhibition and neurite repulsion (Fournier et al., 2000; Luo et al., 1993; Montani et al., 2009). Our in vitro results are best explained by an anti-adhesive/repulsive cell surface action of Nogo-A on

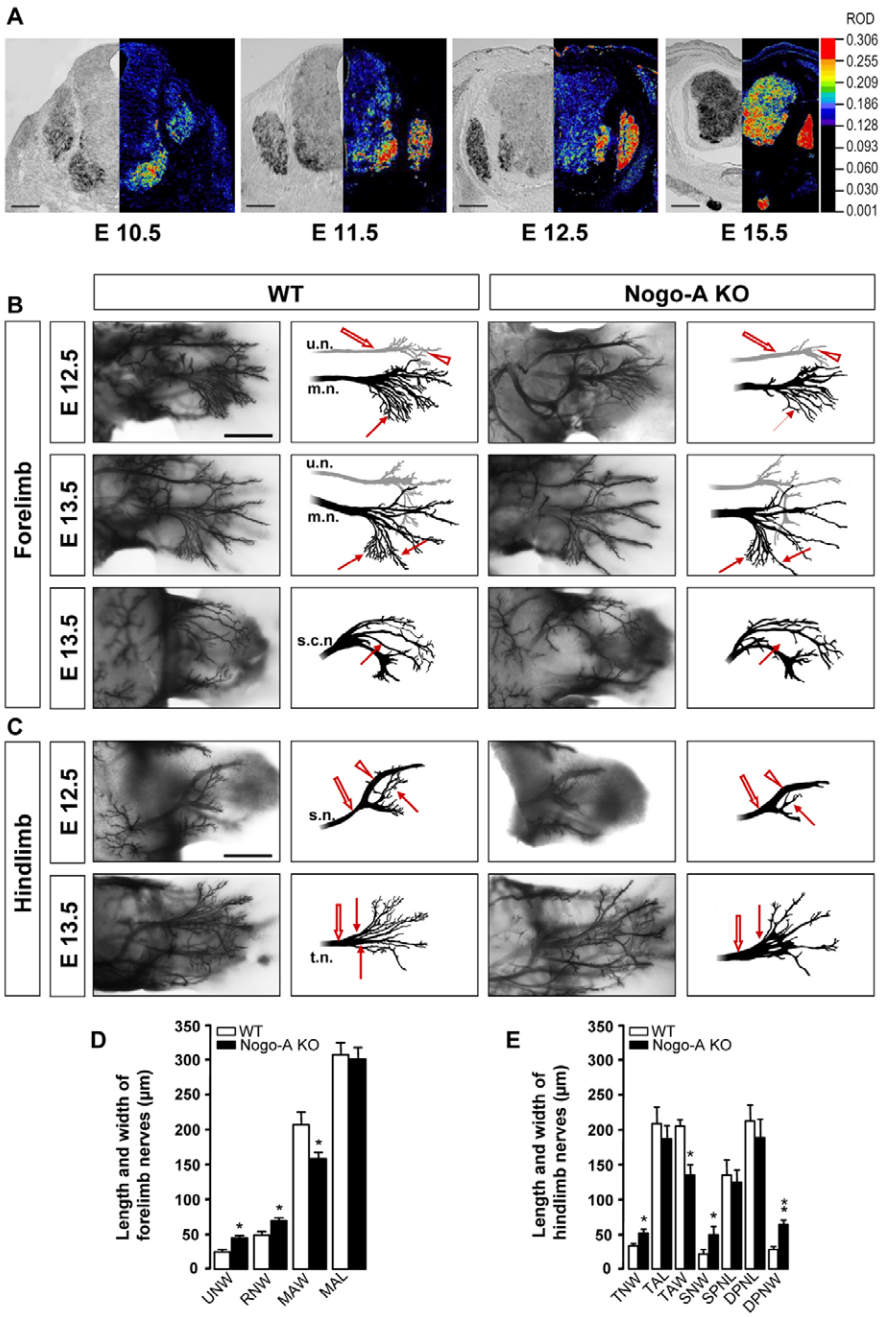

Fig. 7. Nogo-A KO mouse embryos show defects in the development of fore- and hindlimb innervation. (**A**) Expression of *Nogo-A* during mouse spinal cord development shown by in situ hybridization. *Nogo-A* mRNA is present in sensory neurons of dorsal root ganglia and motoneurons in the lumbar spinal cord of the E10.5 mouse embryo. Expression of *Nogo-A* increases until E15.5. ROD, relative optical density. Scale bars: 100 μm, E10.5-E12.5; 200 μm, E15.5. (**B**) Whole-mount anti-neurofilament 160 immunostaining of wild-type and Nogo-A KO forelimbs at E12.5 and E13.5. At E12.5, thickness of the ulnar nerve was slightly increased in Nogo-A KO embryos (open arrows, upper panel), whereas its branching was decreased (open arrowhead, upper panel). Branching of the median nerve arbour was markedly reduced at both E12.5 and E13.5 in Nogo-A KO embryos (arrows, upper and middle panels). At E13.5, a reduction in the branching pattern of sensory cutaneous nerves was apparent; both major and fine branches were missing (arrow, lower panel). u.n., ulnar nerve; m.n., median nerve; s.c.n., sensory cutaneous nerves. Scale bar: 150 μm. (**C**) Innervation of wild-type and Nogo-A KO hindlimbs at E12.5 and E13.5. The width of the sciatic nerve and of its deep peroneal branch were increased in the absence of Nogo-A (open arrow and arrowhead, respectively; upper panel), whereas branching of the superficial peroneal nerve was reduced (arrow; upper panel). At E13.5, the tibial nerve divides into two major nerve trunks in wild-type embryos (arrows, lower panel). This bifurcation of the tibial nerve was disrupted in the absence of Nogo-A (arrow; lower panel) and its thickness was increased (open arrows, lower panel). s.n., sciatic nerve; t.n., tibial nerve. Scale bar: 150 μm. (**D**) Quantitation of the length and width of forelimb innervating nerves in wild-type and Nogo-A KO E13.5 embryos. UNW, ulnar nerve width; RNW, radial nerve width; MAW, median nerve arbour width; MAL, median nerve arbour length. Values represent means ± s.e.m. of 12 embryos per condition; **P*<0.05, Student's *t*-test. (**E**) Quantitation of the length and width of hindlimb innervating nerves in wild-type and Nogo-A KO E13.5 embryos. TNW, tibial nerve width; TAL, tibial nerve arbour length; TAW, tibial nerve arbour width; SNW, sciatic nerve width; SPNL, superficial peroneal nerve length; DPNL, deep peroneal nerve length; DPNW, deep peroneal nerve width. Values represent means ± s.e.m. of 12 embryos per condition; **P*<0.05 and ***P*<0.01, Student's *t*-test.

neighbouring neurites and cells. Fasciculation and branching are crucially dependent upon adhesive and repulsive interactions between the neurites themselves, as well as with the surrounding tissue and matrix components. Removal or inactivation of Nogo-A or Nogo-A signalling, e.g. by blocking the active site or by sterically interfering with ligand-receptor binding by a bulky IgG antibody binding to sequences of Nogo-A or of the receptor components NgR or Lingo1, lead to exaggerated adhesion and, thereby, increased fasciculation in the dense neurite plexus of DRG explant cultures and of growing peripheral nerves in embryos in vivo. Unbalanced adhesive interactions might also be responsible for the fact that many neurites were unable to leave the sciatic plexus in the chicken embryos injected with anti-Nogo-A antibodies; within the plexus region, bundles of motor and sensory axons need to defasciculate in order to form the new fascicles destined to innervate individual muscle groups (Milner et al., 1998; Tosney and Landmesser, 1985). Likewise, the inability of neurites to leave a fibre bundle could be responsible for the conspicuous absence of branches of limb nerves in antibody-treated chicken and in Nogo-A KO mouse embryos. Muscle nerve formation in *Drosophila* is crucially dependent on defasciculation (Van Vactor, 1998). In the chicken embryo, removal of the repulsive component PSA from NCAM resulted in an increased bundling of axons and a concomitant failure of branching of peripheral nerves (Landmesser et al., 1990; Rafuse and Landmesser, 2000; Tang et al., 1992; Tang et al., 1994). Controlled adhesion/repulsion seems therefore to be essential for the ability of neurites to form branches and/or for the ability of branches to leave a fascicle or its parent neurite. Interestingly, a marked decrease of branch formation was also seen in dissociated DRG neurons cultured at single-cell density. The increase in the length of the individual neurites corresponded to the decrease in the number of branches (identical total neurite length per cell). Repulsive interactions between dividing growth cones or branch sprouts and the parent neurite were suggested for repulsors such as ephrins (McLaughlin et al., 2003), and slit is known to enhance branch formation of ingrowing sensory fibres in the developing spinal cord (Wang et al., 1999). The almost 90° angles formed by many branches are consistent with an important role of repulsive interactions between growing processes of a single neuron. These branch angles were significantly smaller in Nogo-A KO or antibody-treated cells, suggesting that Nogo-A is an important repulsive factor required for branch formation and branch direction. The clear segregation observed when wild-type and Nogo-A KO dissociated DRG neurons were mixed is consistent with differences in adhesive/repulsive cell surface properties exerted non-cell autonomously in trans during cell-cell interactions. However, owing to other players and possible compensations, the detailed mechanism could be complex.

In DRG cultures, neutralization of the Nogo-A receptor components NgR or Lingo1 by the respective antibodies, or blockade of the Rho effector ROCK by the Y27632 compound, phenocopied the results observed after Nogo-A neutralization or KO, thus suggesting an NgR-Rho/ROCK-dependent mechanism of action for Nogo-A in neurite fasciculation and branching. In vivo, the acute downregulation of Nogo-A in embryonic chick hindlimbs also caused major defects of peripheral nerve formation. Although inhibition of the Rho effector ROCK in vivo did not reproduce the full extent of the phenotype seen after inhibition of Nogo-A by function-blocking antibody, the observed phenotype is consistent with a role of ROCK signalling downstream of Nogo-A. Thus, both Nogo-A and ROCK are required for the sorting of axons in the sciatic plexus of the developing hindlimb. The analysis of fore- and hindlimb peripheral nerves in Nogo-A KO mouse embryos showed missing branches and thicker nerves, although unlike in the chicken embryo, most main nerve trunks were present in the Nogo-A KO embryos. These characteristic changes were mostly transient and no longer observed at E15.5 (see Fig. S9 in the supplementary material). However, at late developmental stages only major defects can be readily and reproducibly observed and quantified. The less severe phenotype of Nogo-A KO mice compared with that of anti-Nogo-A antibody-injected chicken embryos might also be related to a compensatory upregulation of other repulsive molecules. Indeed, increased levels of mRNA or protein for several ephrins and semaphorins, and for some of their receptors, have been observed in Nogo-A KO mice (data not shown). Although in adult Nogo-A KO mice Nogo-A deletion resulted in Nogo-B upregulation, this was not the case during embryonic development (see Fig. S10 in the supplementary material). Nogo-A was also weakly expressed by embryonic muscles at that age. There, it might provide additional help in keeping the growing axons en route by forming a repulsive environment. Absence of muscle Nogo-A would then lead to defasciculation and aberrant branching; however, such a phenotype was not observed here, indicating that Nogo-A on the neurons and neurites themselves might play the more important role.

The present results show a key role of Nogo-A/Nogo receptor signalling in fascicle formation and branching of developing peripheral neurons in vitro and in vivo. The observations are best explained by repulsive/anti-adhesive effects exerted by cell surface Nogo-A via the Nogo receptor complex and Rho-ROCK activation. These effects counter-balance adhesive/attractive interactions in the concert of axonal guidance adhesion, and recognition molecules and mechanisms. Nogo-A thus joins the families of developmental repulsive/inhibitory regulators of neurite growth. As development proceeds, Nogo-A assumes a function as a growth restrictor and stabilizer of the maturing and adult nervous system, whereby its expression shifts to oligodendrocytes and the CNS becomes its main site of action (Gonzenbach and Schwab, 2008; Huber et al., 2002).

Acknowledgements

We are grateful to Roland Schoeb and Eva Hochreutener for help with image processing. We would also like to thank Sandrine Joly for help with qRT-PCR and Eva Riegler for help with the chicken in vivo experiments. This work was supported by the Swiss National Science Foundation (31-63633.00), the NCCR Neural Plasticity and Repair, and the EU Framework 6 Network of Excellence NeuroNE.

Competing interests statement

The authors declare no competing financial interests.

Supplementary material

Supplementary material for this article is available at
http://dev.biologists.org/lookup/suppl/doi:10.1242/dev.048371/-/DC1

References

Aloy, E. M., Weinmann, O., Pot, C., Kasper, H., Dodd, D. A., Rulicke, T., Rossi, F. and Schwab, M. E. (2006). Synaptic destabilization by neuronal Nogo-A. *Brain Cell Biol.* **35**, 137-156.

Bandtlow, C. and Dechant, G. (2004). From cell death to neuronal regeneration, effects of the p75 neurotrophin receptor depend on interactions with partner subunits. *Sci. STKE* **2004**, pe24.

Bouquet, C., Soares, S., von Boxberg, Y., Ravaille-Veron, M., Propst, F. and Nothias, F. (2004). Microtubule-associated protein 1B controls directionality of growth cone migration and axonal branching in regeneration of adult dorsal root ganglia neurons. *J. Neurosci.* **24**, 7204-7213.

Caroni, P. and Schwab, M. E. (1988). Antibody against myelin-associated inhibitor of neurite growth neutralizes nonpermissive substrate properties of CNS white matter. *Neuron* **1**, 85-96.

Chen, M. S., Huber, A. B., van der Haar, M. E., Frank, M., Schnell, L., Spillmann, A. A., Christ, F. and Schwab, M. E. (2000). Nogo-A is a myelin-associated neurite outgrowth inhibitor and an antigen for monoclonal antibody IN-1. *Nature* **403**, 434-439.
Chilton, J. K. (2006). Molecular mechanisms of axon guidance. *Dev. Biol.* **292**, 13-24.
Dickson, B. J. (2002). Molecular mechanisms of axon guidance. *Science* **298**, 1959-1964.
Dimou, L., Schnell, L., Montani, L., Duncan, C., Simonen, M., Schneider, R., Liebscher, T., Gullo, M. and Schwab, M. E. (2006). Nogo-A-deficient mice reveal strain-dependent differences in axonal regeneration. *J. Neurosci.* **26**, 5591-5603.
Dodd, D. A., Niederoest, B., Bloechlinger, S., Dupuis, L., Loeffler, J. P. and Schwab, M. E. (2005). Nogo-A, -B, and -C are found on the cell surface and interact together in many different cell types. *J. Biol. Chem.* **280**, 12494-12502.
Eberhart, J., Swartz, M., Koblar, S. A., Pasquale, E. B., Tanaka, H. and Krull, C. E. (2000). Expression of EphA4, ephrin-A2 and ephrin-A5 during axon outgrowth to the hindlimb indicates potential roles in pathfinding. *Dev. Neurosci.* **22**, 237-250.
Fournier, A. E., Kalb, R. G. and Strittmatter, S. M. (2000). Rho GTPases and axonal growth cone collapse. *Methods Enzymol.* **325**, 473-482.
Fournier, A. E., GrandPre, T. and Strittmatter, S. M. (2001). Identification of a receptor mediating Nogo-66 inhibition of axonal regeneration. *Nature* **409**, 341-346.
Fournier, A. E., Takizawa, B. T. and Strittmatter, S. M. (2003). Rho kinase inhibition enhances axonal regeneration in the injured CNS. *J. Neurosci.* **23**, 1416-1423.
Gonzenbach, R. R. and Schwab, M. E. (2008). Disinhibition of neurite growth to repair the injured adult CNS: focusing on Nogo. *Cell. Mol. Life Sci.* **65**, 161-176.
Hamburger, V. and Hamilton, H. L. (1951). A series of normal stages in the development of the chick embryo. *J. Morphol.* **88**, 49-92.
Huber, A. B., Weinmann, O., Brosamle, C., Oertle, T. and Schwab, M. E. (2002). Patterns of Nogo mRNA and protein expression in the developing and adult rat and after CNS lesions. *J. Neurosci.* **22**, 3553-3567.
Huber, A. B., Kania, A., Tran, T. S., Gu, C., De Marco Garcia, N., Lieberam, I., Johnson, D., Jessell, T. M., Ginty, D. D. and Kolodkin, A. L. (2005). Distinct roles for secreted semaphorin signaling in spinal motor axon guidance. *Neuron* **48**, 949-964.
Hunt, D., Coffin, R. S., Prinjha, R. K., Campbell, G. and Anderson, P. N. (2003). Nogo-A expression in the intact and injured nervous system. *Mol. Cell. Neurosci.* **24**, 1083-1102.
Josephson, A., Widenfalk, J., Widmer, H. W., Olson, L. and Spenger, C. (2001). NOGO mRNA expression in adult and fetal human and rat nervous tissue and in weight drop injury. *Exp. Neurol.* **169**, 319-328.
Kalil, K., Szebenyi, G. and Dent, E. W. (2000). Common mechanisms underlying growth cone guidance and axon branching. *J. Neurobiol.* **44**, 145-158.
Kapfhammer, J. P. and Schwab, M. E. (1994). Inverse patterns of myelination and GAP-43 expression in the adult CNS: neurite growth inhibitors as regulators of neuronal plasticity? *J. Comp. Neurol.* **340**, 194-206.
Landmesser, L., Dahm, L., Schultz, K. and Rutishauser, U. (1988). Distinct roles for adhesion molecules during innervation of embryonic chick muscle. *Dev. Biol.* **130**, 645-670.
Landmesser, L., Dahm, L., Tang, J. C. and Rutishauser, U. (1990). Polysialic acid as a regulator of intramuscular nerve branching during embryonic development. *Neuron* **4**, 655-667.
Liebscher, T., Schnell, L., Schnell, D., Scholl, J., Schneider, R., Gullo, M., Fouad, K., Mir, A., Rausch, M., Kindler, D. et al. (2005). Nogo-A antibody improves regeneration and locomotion of spinal cord-injured rats. *Ann. Neurol.* **58**, 706-719.
Luo, Y., Raible, D. and Raper, J. A. (1993). Collapsin: a protein in brain that induces the collapse and paralysis of neuronal growth cones. *Cell* **75**, 217-227.
Maina, F., Hilton, M. C., Ponzetto, C., Davies, A. M. and Klein, R. (1997). Met receptor signaling is required for sensory nerve development and HGF promotes axonal growth and survival of sensory neurons. *Genes Dev.* **11**, 3341-3350.
McGee, A. W., Yang, Y., Fischer, Q. S., Daw, N. W. and Strittmatter, S. M. (2005). Experience-driven plasticity of visual cortex limited by myelin and Nogo receptor. *Science* **309**, 2222-2226.
McLaughlin, T., Hindges, R., Yates, P. A. and O'Leary, D. D. (2003). Bifunctional action of ephrin-B1 as a repellent and attractant to control bidirectional branch extension in dorsal-ventral retinotopic mapping. *Development* **130**, 2407-2418.
Mi, S., Lee, X., Shao, Z., Thill, G., Ji, B., Relton, J., Levesque, M., Allaire, N., Perrin, S., Sands, B. et al. (2004). LINGO-1 is a component of the Nogo-66 receptor/p75 signaling complex. *Nat. Neurosci.* **7**, 221-228.
Milner, L. D., Rafuse, V. F. and Landmesser, L. T. (1998). Selective fasciculation and divergent pathfinding decisions of embryonic chick motor axons projecting to fast and slow muscle regions. *J. Neurosci.* **18**, 3297-3313.
Mingorance-Le Meur, A., Zheng, B., Soriano, E. and del Rio, J. A. (2007). Involvement of the myelin-associated inhibitor Nogo-A in early cortical development and neuronal maturation. *Cereb. Cortex* **17**, 2375-2386.
Montani, L., Gerrits, B., Gehrig, P., Kempf, A., Dimou, L., Wollscheid, B. and Schwab, M. E. (2009). Neuronal Nogo-A modulates growth cone motility via Rho-GTP/LIMK1/cofilin in the unlesioned adult nervous system. *J. Biol. Chem.* **284**, 10793-10807.
Oertle, T., van der Haar, M. E., Bandtlow, C. E., Robeva, A., Burfeind, P., Buss, A., Huber, A. B., Simonen, M., Schnell, L., Brosamle, C. et al. (2003). Nogo-A inhibits neurite outgrowth and cell spreading with three discrete regions. *J. Neurosci.* **23**, 5393-5406.
Perrin, F. E. and Stoeckli, E. T. (2000). Use of lipophilic dyes in studies of axonal pathfinding in vivo. *Microsc. Res. Tech.* **48**, 25-31.
Pourquie, O., Coltey, M., Thomas, J. L. and Le Douarin, N. M. (1990). A widely distributed antigen developmentally regulated in the nervous system. *Development* **109**, 743-752.
Rafuse, V. F. and Landmesser, L. T. (2000). The pattern of avian intramuscular nerve branching is determined by the innervating motoneuron and its level of polysialic acid. *J. Neurosci.* **20**, 1056-1065.
Rutishauser, U. (2008). Polysialic acid in the plasticity of the developing and adult vertebrate nervous system. *Nat. Rev. Neurosci.* **9**, 26-35.
Rutishauser, U., Gall, W. E. and Edelman, G. M. (1978). Adhesion among neural cells of the chick embryo. IV. Role of the cell surface molecule CAM in the formation of neurite bundles in cultures of spinal ganglia. *J. Cell Biol.* **79**, 382-393.
Schaeren-Wiemers, N. and Gerfin-Moser, A. (1993). A single protocol to detect transcripts of various types and expression levels in neural tissue and cultured cells: in situ hybridization using digoxigenin-labelled cRNA probes. *Histochemistry* **100**, 431-440.
Schwab, M. E. (2004). Nogo and axon regeneration. *Curr. Opin. Neurobiol.* **14**, 118-124.
Simonen, M., Pedersen, V., Weinmann, O., Schnell, L., Buss, A., Ledermann, B., Christ, F., Sansig, G., van der Putten, H. and Schwab, M. E. (2003). Systemic deletion of the myelin-associated outgrowth inhibitor Nogo-A improves regenerative and plastic responses after spinal cord injury. *Neuron* **38**, 201-211.
Tang, J., Landmesser, L. and Rutishauser, U. (1992). Polysialic acid influences specific pathfinding by avian motoneurons. *Neuron* **8**, 1031-1044.
Tang, J., Rutishauser, U. and Landmesser, L. (1994). Polysialic acid regulates growth cone behavior during sorting of motor axons in the plexus region. *Neuron* **13**, 405-414.
Tosney, K. W. and Landmesser, L. T. (1985). Development of the major pathways for neurite outgrowth in the chick hindlimb. *Dev. Biol.* **109**, 193-214.
Van Vactor, D. (1998). Adhesion and signaling in axonal fasciculation. *Curr. Opin. Neurobiol.* **8**, 80-86.
Wang, G. and Scott, S. A. (2000). The "waiting period" of sensory and motor axons in early chick hindlimb: its role in axon pathfinding and neuronal maturation. *J. Neurosci.* **20**, 5358-5366.
Wang, K. H., Brose, K., Arnott, D., Kidd, T., Goodman, C. S., Henzel, W. and Tessier-Lavigne, M. (1999). Biochemical purification of a mammalian slit protein as a positive regulator of sensory axon elongation and branching. *Cell* **96**, 771-784.
Wang, X., Chun, S. J., Treloar, H., Vartanian, T., Greer, C. A. and Strittmatter, S. M. (2002). Localization of Nogo-A and Nogo-66 receptor proteins at sites of axon-myelin and synaptic contact. *J. Neurosci.* **22**, 5505-5515.
Yiu, G. and He, Z. (2006). Glial inhibition of CNS axon regeneration. *Nat. Rev. Neurosci.* **7**, 617-627.